Chemical composition of fluid inclusions in Colombian emerald deposits

G. Giuliani[1*], A. Cheilletz[2,3], J. Dubessy[4] and C. T. Rodriguez[5]

[1] ORSTOM, University of Brasília, 70910 Brasília DF, Brazil
[2] C.R.P.G., BP 20, 54501 Vandoeuvre Cedex, France
[3] E.N.S.G., BP 452, 54001 Nancy Cedex, France
[4] CREGU, BP 23, 54501 Vandoeuvre Cedex, France
[5] MINERALCO S.A., calle 32, N°13-07, Apartado 17878, Bogotà, Colombia

With 7 figures

Abstract. The chemical composition of fluid inclusions in emerald deposits from Colombia was investigated by microthermometry, scanning electron microscopy and Raman spectrometry. Fluid inclusions in emerald can be subdivided into two types: type 1 corresponds to halite-saturated fluid inclusions containing a cubic crystal of halite (12–15 vol.%), a brine (75 vol.%) and a gas phase (10–13 vol.%); type 2 are daughter mineral-rich fluid inclusions with NaCl, KCl, (Ca, Fe)Cl mixtures and various carbonate phases. The vapour phase is composed of H_2O, CO_2, and N_2 in variable proportions.

The mineralizing fluid is interpreted as homogeneous and hypersaline, and belongs to the H_2O-$NaCl$-$CaCl_2$-KCl-CO_2-N_2 system. The salt components may derive from leaching of the evaporitic strata interbedded within the Lower Cretaceous series; the CO_2, N_2, and Ca components may be related to the black shale wall rocks.

Introduction

The genesis of the emerald deposits of Colombia can be related to an epigenetic hydrothermal process confined to the black shale series of the Eastern Cordillera (Forero, 1987). Previous fluid inclusion studies have demonstrated that the paleofluids involved in the genesis of emeralds are commonly of high salinity and great complexity (Gubelin, 1957; Touray & Poirot, 1968; Roedder, 1963; 1972). A total salinity of 40 wt.% eq. NaCl was reported by Kozlowski et al. (1988) whereas halite daughter crystals were identified as solid trapped phases (Roedder, 1982). Gas species are limited to H_2O, CO_2, and N_2 (Rosasco & Roedder, 1979; Dele-Dubois et al., 1980).

The present paper provides new fluid inclusion data on Colombian emerald mineralizations using combined microthermometry, Raman spectroscopy and scanning electron microscopy (SEM).

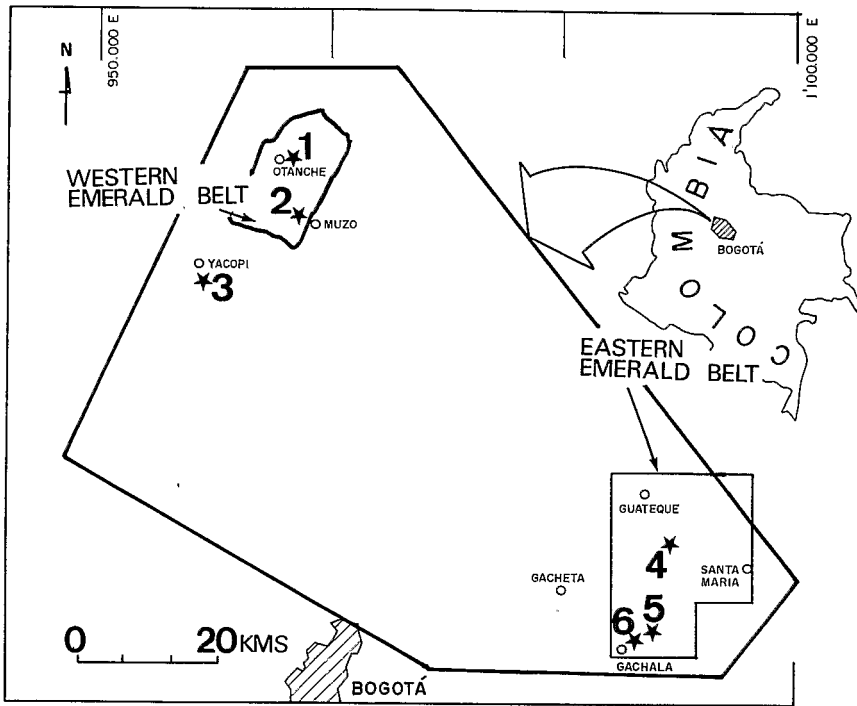* Present address: C.R.P.G., BP 20, 54501 Vandoeuvre Cedex, France

Fig. 1. Location of the emerald mines studied in the Eastern Colombian Cordillera. 1=Coscuez; 2=Quipama, Tequendama, Las Pavas; 3=Yacopi-La Mina; 4=Chivor; 5=Las Cruces, El Diamante, El Toro; 6=La Vega San Juan.

Geological setting

The Colombian emerald deposits are located in two narrow belts within the Eastern Cordillera (Fig. 1). The eastern belt comprises the districts of Gachalà (Vega San Juan, Las Cruces, El Diamante, El Toro mines) and Chivor. The western belt encloses the districts of Coscuez, Muzo (Quipama, Tequendama, Porto-Arturo, Solis-Pavas mines) and La Palma-Yacopí. The deposits, hosted by Lower Cretaceous marine shales of the Eastern Cordillera, are located at the intersection of two regional lineaments: a NE-SW steep reverse fault system and a NW-SE fault system (United Nations – Ingeominas, 1975).

Extensive brecciation and stratabound mineralization are the result of hydraulic fracturing, which is one of the main factors controlling emerald mineralization (Giuliani et al., 1990). In both districts, emeralds occur in calcite-dolomite veins, up to 10 cm thick, pockets and brecciated zones. The gangue consists of variable proportions of albite, quartz, fluorite, pyrite, baryte, REE-carbonates, and parisite [$F_2(Ce, La)CaCO_3$] which was first discovered in the Muzo district. Emerald is generally observed in drusy cavities.

Metasomatic hydrothermal alteration of the black shales has developed around the emerald veins and is characterized by an intense albitization and carbonatization halo (Beus, 1979). Major

and trace element geochemistry of the metasomatic zones reflects the leaching of K_2O, SiO_2, Al_2O_3, Ba, Rb, Cr, V, and Th (Giuliani et al., 1990).

Samples were collected in the western belt, in the Coscuez, Muzo and La Palma-Yacopí districts, and in the eastern belt, in the Gachalà and Chivor districts (Fig. 1). Emerald crystals and the commonly associated minerals, quartz, fluorite, and pyrite, were sampled from veins, pockets and breccias.

Analytical methods

Microscopic observations: The distribution and general features of fluid inclusions were first examined under the microscope in doubly-polished thin sections.

Scanning electron microscopy (SEM): Thin sections of various crystals were fractured and fixed to a support with lacquer. The specimen, covered by a thin conducting film of evaporated carbon, was examined with a Cambridge Stereoscan 250 scanning electron microscope, using an accelerating voltage of 25 kV.

Raman spectroscopy: Spectra were obtained on a Dilor X-Y multichannel laser-excited Raman spectrometer using the 514.5 nm radiation of an Ar ion laser (Spectra-Physics type 2020). The general methodology was described by Dubessy et al. (1989).

Microthermometry: Fluid inclusions contained in emerald from the Vega San Juan mine were studied using microthermometry. It was performed on doubly-polished plates using a Chaix-Méca heating-freezing stage.

Results

Fluid inclusion petrography

Microscopic observations of thin sections in emerald show that the paleofluids trapped as primary or secondary fluid inclusions can be subdivided into two types: type 1 corresponds to halite-saturated fluid inclusions containing a cubic crystal of halite (12–15 vol.%), a brine (75 vol.%) and a gas phase (10–13 vol.%); type 2 corresponds to daughter mineral-rich fluid inclusions with NaCl, KCl and various others salts.

Generally, a liquid carbonic phase is only visible in flat inclusions (LCO_2 up to 3% of the total cavity volume) or is clearly indicated by the formation of solid CO_2 and a clathrate during freezing experiments. Liquid carbon dioxide was not found in the Vega San Juan deposit. Type 2 fluid inclusions are characterized by the presence of other daughter minerals such as sylvite, complex (Fe, Ca)Cl salt mixtures, carbonates, sulphides, silicates and iron oxides.

Chemical composition of fluid inclusions

Raman spectroscopy data

The Raman spectra of the gas phase of emerald fluid inclusions from all the deposits, except the Vega San Juan mine, yield a strong peak for CO_2 (1388 cm⁻¹) and, occasionally, an additional peak
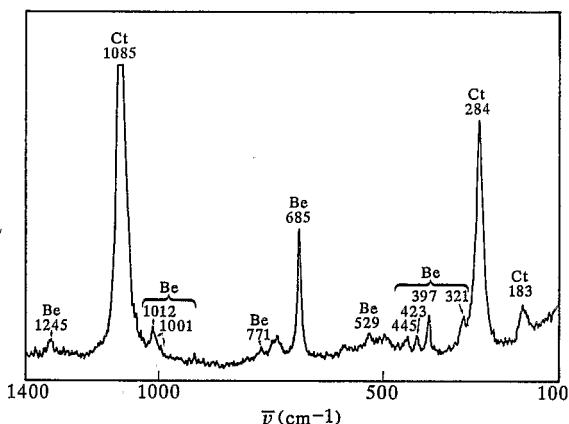
Fig. 2. La Vega San Juan deposit: Raman spectrum of calcite in a fluid inclusion in emerald. Ct=calcite; Be=host emerald.
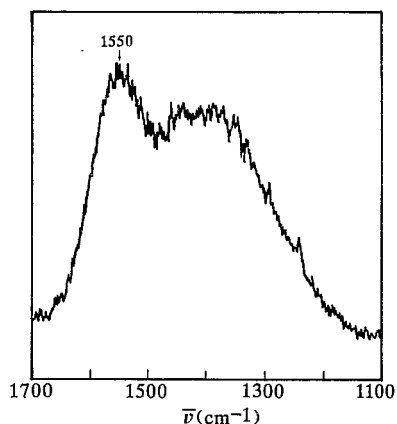
Fig. 3. La Vega San Juan deposit: Raman spectrum of a carbonaceous compound in a fluid inclusion.

at 2330 cm^{-1} assigned to N_2 which has already been documented by Dele-Dubois et al. (1980). Raman spectra of brines show no dissolved species such as CO_2, HCO_3^-, CO_3^{2-} and SO_4^{2-}.

Raman spectra obtained on the daughter mineral-bearing fluid inclusions identified calcite as a main daughter mineral (Fig. 2) with the following peaks: 157.9, 283.8, 736, and 1085.1 cm^{-1}. The spectra of the calcite crystals associated with emeralds in the same deposits are characterized by the 158.0, 283.8, 713.2, and 1086.9 cm^{-1} peaks. The deviation registered for the position of the peaks and particularly the presence of the 736 cm^{-1} peak for the calcite daughter mineral, is probably related to variations in the chemical composition of the daughter carbonates. Indeed, SEM data revealed complex Ca-Fe-Zn carbonates in the cavity of fluid inclusions.

In the Vega San Juan deposit, a poorly organized carbonaceous compound was identified by its characteristic spectrum (Fig. 3), a strong and wide band at 1350 to 1400 cm^{-1}. The E2g band usually located around 1600 cm^{-1} in kerogen compounds (Bény-Bassez et al., 1981) is, in this case, situated at 1550 cm^{-1}. This suggests that these carbonaceous compounds did not evolve by a simple thermal maturation process.

Scanning electron microscopy data

The daughter minerals of the fluid inclusions in emeralds from all the mines studied were investigated by SEM. Different complex mixed salts and minerals were identified.

NaCl and KCl, in variable amounts, are the most frequent daughter minerals found in emeralds. The association NaCl-KCl is frequent in the Coscuez and Muzo mines (Figs. 4a; 5c, d). Complex salt mixtures are also frequent in all the districts: Cl(Ca, Fe) salts (Fig. 6); Cl(Fe, K, Ca); Cl(Fe, Mn, Ca, K); Cl(K, Fe, Mn); Cl(K, Fe), Cl(Ca, K, Fe, Cr); Cl(K, Ca).

Other daughter minerals include carbonates: Zn-Ca ; Ca-Fe or Ca-Fe-Mg (dolomite); Ca-La-Ce (parisite); Fe (siderite); sulphides: Fe-S (pyrite); Zn-S (sphalerite); silicates: Si-Ca-Ti-Fe (titanite); Si-Al (emerald); Si-K-Al (K-mica); Si (quartz); iron oxides: (Fe); and apatite (Ca-P).
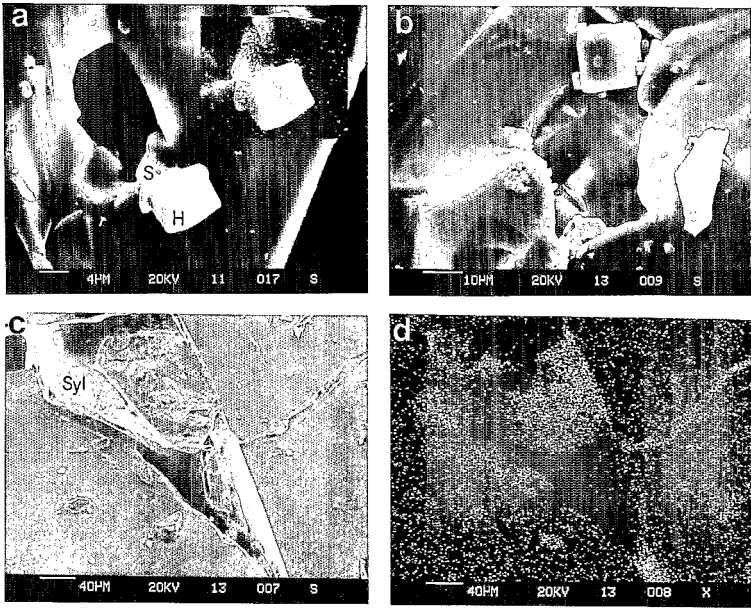
Fig. 4. Coscuez deposit: a – SEM microphotograph of halite (H) and sylvite (S) in a cavity of emerald fluid inclusion with superposition of the K electron map for the corresponding salts. b – Cubic halite crystal in a cavity of fluid inclusion in emerald. c – Sylvite crystal (Syl) from a cavity in pyrite. d – Backscattered electron map (Ca) of the decrepitate representative of the brine-bearing fluid inclusion.
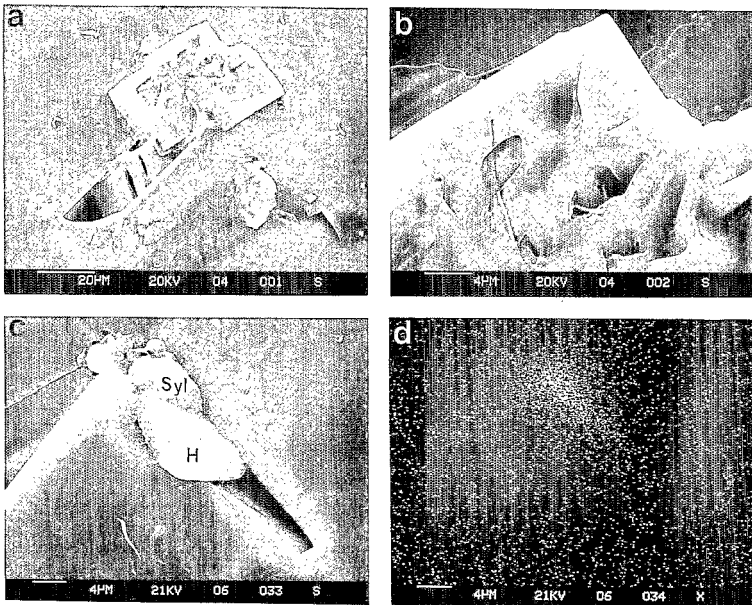

Fig. 5. La Vega deposit: a – and b – SEM microphotographs of halite crystal from fluid inclusion in emerald. c – Characteristic association of halite (H) and sylvite (Syl) in emerald. d – K distribution within the inclusion of Fig. 5c.
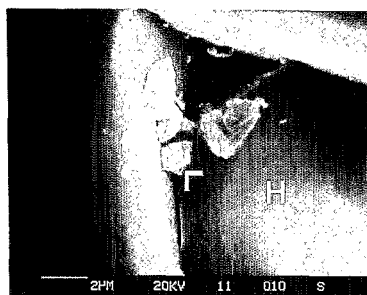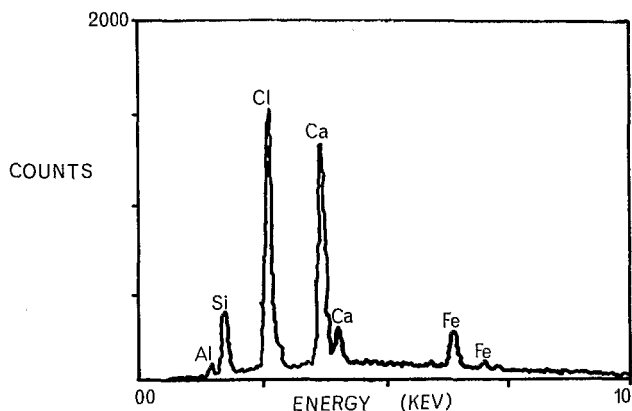
Fig. 6. Coscuez deposit: SEM microphotograph of (Ca, Fe)Cl daughter minerals in a fluid inclusion cavity in emerald and its SEM energy dispersive spectrum; H=halite.

Primary fluid inclusions of up to 400 μm, containing sylvite daughter mineral, were encountered in pyrite crystals from the Coscuez deposit (Fig. 4c). Opening these fluid inclusion cavities during electron beam impact permitted to evaporate the infilling brine and to analyze the decrepitate, which appeared to consist of a mixture of Ca-Cl composition (Fig. 4d).

Microthermometric data

In the Vega San Juan deposit, the trapped fluids are typical Type 1 fluid inclusions; at room temperature KCl is less frequent than NaCl (Fig. 5). On cooling, eutectic temperatures ranging from −56.1°C to −52°C and final melting of ice from −35.3°C to −31.6°C, clearly confirm the presence of Ca^{2+} in significant amount in the solution (Crawford, 1981). Traces of CO_2 in the gas phase were only detected in a few cases by Raman spectrometry but on freezing, neither solidification of liquid CO_2 nor nucleation of a clathrate were detected.

During freezing experiments, the nucleation of solids which grew in NaCl crystal-bearing fluid inclusions, is common as indicated by Roedder (1963), and Touray & Poirot (1968). These solids nucleate during each cooling cycle and are metastable at laboratory temperature. They are anisotropic with a moderate relief, and measure up to 10 μm (Fig. 7a). On heating, their melting temperatures range between +50° and +284°C. Therefore, these solids can be considered as hydrates. In the Coscuez emerald sample, Raman spectrometry allowed the characterization of these hydrates which are defined by their lines at 3416, 1634, and 1653 cm⁻¹ (Fig. 7b). There

Fig. 7. Coscuez deposit: a – Typical three-phase fluid inclusion in emerald. L=brine; V=vapour phase; H=halite crystal; h=metastable hydrate. b – Hydrate Raman spectra obtained at +20°C. The melting temperature of this hydrate was measured at +139°C.
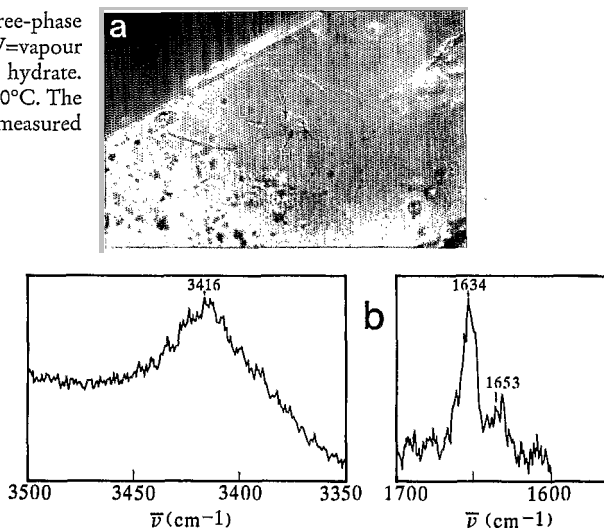
are no data available on hydrates of geological interest (Dubessy et al., 1982) to permit their identification. However, the presence of a hydrate in the fluid associated with emerald deposition suggests the existence of additional ions (Fe, Mg, Ca) in the brine.

On heating, decrepitation and leakage characterize the majority of the fluid inclusions. Halite crystals dissolution occurs at temperatures ranging from +284° to +326°C (mode= +300°C). However, many halite crystals remain undissolved at the temperatures of decrepitation which ranges from +205° to +333°C. Homogenization temperatures in the liquid state (T_h) range between +215° and +330°C with a significant mode at +235°C. Dissolution of the Ca-Fe chlorides ranges from +233° to +284°C. According to Vanko et al. (1988), the combined temperature of halite dissolution (T_s) and the final melting of ice give, in the absence of CO_2, an estimated total salinity of the fluid of $(H_2O)_{55}$-$(NaCl)_{30}$-$(CaCl_2)_{15}$.
Saturation of the fluid with respect to NaCl is indicated by $T_s>T_h$ and the existence of fissural deposition of halite crystals in emerald. This can be due to the injection of hypersaline brines causing salt crystallization during cooling. Frequent necking-down processes can also be advocated to explain the large halite volume in relation to the total volume of cavities.

P-T trapping conditions have been evaluated as follows: the trapping temperature can be estimated by using the modal melting temperature of halite (T_s=300°C), considering an average homogeneous brine $(H_2O)_{55}$-$(NaCl)_{45}$. The corresponding isochore using the Brown & Lamb (1989) calculation program allows the trapping pressure (P=1.5 kb) to be estimated. One should remember, however, that the presence of $CaCl_2$ components in the fluid will lower this P-T estimate (Steward & Potter, 1979).

The estimated trapping pressure can be confirmed by examining the decrepitation conditions. Most inclusions larger than 20 µm decrepitate or leak before total homogenization. Leakage varies with the internal fluid pressure in relation to the nature and the density of the fluid filling the inclusion, as well as the size and the nature of the mineral (Roedder, 1984). The decrepitation curve for beryl is unknown; considering that beryl and quartz have comparable hardnesses, estimated internal fluid pressure at the decrepitation temperature (for ≈20 µm inclusions) is approximately 1 kb (Roedder, 1984), near the estimated isochoric trapping pressure.

Discussion and conclusions

The main benefit of this work is a significantly improved characterization of hypersaline fluids in the Colombian emerald deposits. A combined microthermometric-Raman-SEM analysis show that these fluids contain H_2O, $NaCl$, $CaCl_2$, KCl, CO_2, and N_2. In the Vega San Juan deposit, uniform T_s data and the abundance of trapped halite crystals show that the fluid was saturated with respect to $NaCl$ at the time of trapping. Another important outcome is the evidence obtained regarding fluid composition homogeneity in the different emerald districts.

Current models on the origin of Colombian emerald deposits are concerned with two main aspects: (1) the origin of beryllium, possibly remobilized from the black shales (Medina, 1970; United Nations – Ingeominas, 1975; Kozlowski et al., 1988) or transported upward by hydrothermal fluids (Oppenheim, 1948; Beus & Mineev, 1972; Guerrero & Villanueva, 1986), and (2) the origin of the mineralizing fluids, which may have been derived from connate waters (Medina, 1970), or related to hydrothermal circulation either at low (Beus & Mineev, 1972) or high temperatures (Oppenheim, 1948; Guerrero & Villanueva, 1986). Finally, a possible relation with diapiric intrusive saline domes was also suggested (MacLaughlin & Arce, 1971; Kozlowski et al., 1988). The data presented here clearly favour the last of these hypotheses.

Brines containing $NaCl$, KCl, and $CaCl_2$ can result from leaching of evaporitic horizons, which are known to occur interbedded within the Lower Cretaceous shales, by a hot hydrothermal fluid (Kozlowski et al., 1988). In diapiric saline dome environments, the associated fluids belong to the H_2O-$NaCl$-KCl-CO_2-N_2 system (Guilhaumou et al., 1981), the CO_2-N_2 fraction resulting from the oxidation of NH_4^+ and CH_4 (Dubessy & Ramboz, 1986). The large spectrum of similar elements found in the fluids associated with Colombian emerald deposits, together with the P-T estimates and geological environment, are in agreement with the proposed evaporitic origin of the fluids. In fact, saline formations are well known in the Zipaquira and Nemocón regions where emeralds were reported in salt mines (Oppenheim, 1948) and in the Gachalá region (Escovar, 1975). However, in the case of Cretaceous emerald deposits, the source of the CO_2 and N_2 components can simply be ascribed to devolatilization of the black shales.

Similar saline brines are also reported in skarn deposits (Kwak, 1986) associated with high temperature fluid circulation. However, the lack of spatially and temporally associated igneous activity in the Lower Cretaceous series of the Eastern Cordillera of Colombia, as well as the relatively low trapping temperature of the fluid inclusions, preclude any magmatic origin for these brines.

References

Bény-Bassez, C., Rouzaud, J.N. & Oberlin, A., 1981: Premières applications de la microsonde Mole à effet Raman à l'étude d'une série de charbons; C.R. Acad., Sci., Ser. 2, 293, 509–512.

Beus, A.A., 1979: Sodium – a geochemical indicator of emerald mineralization in the Cordillera Oriental, Colombia; J. Geochem. Explor., 11, 195–208.

Beus, A.A. & Mineev, D.A., 1972: Some geological and geochemical features of the Muzo-Coscuez emerald zone, Cordillera Oriental, Colombia; Informe Ingeominas, 1–50 (unpub.).

Brown, P.E. & Lamb, W.M., 1989: PVT properties of fluids in the system $H_2O\pm CO_2\pm NaCl$: new graphical presentations and implications for fluid inclusion studies; Geochim. Cosmochim. Acta, 53, 1209–1221.

Crawford, M.L. 1981: Phase equilibria in aqueous fluid inclusions; in Fluid Inclusions: Applications to Petrology, Short Course Handb., Mineral. Assoc. Can., 6, 75–100.

Dele-Dubois, M.L., Dhamelincourt, P. & Schubnel, H.J., 1980: Étude par spectrométrie Raman d'inclusions dans les diamants, saphirs et émeraudes; Rev. Gemmologie A.F.G., 64, 11–15.

Dubessy, J., Audeoud, D., Wilkins, R. & Kostolanyi, C., 1982: The use of the Raman microprobe Mole in the determination of the electrolytes dissolved in the aqueous phase of fluid inclusions; Chem. Geol., 37, 137–150.

Dubessy, J., Poty, B. & Ramboz, C., 1989: Advances in C-O-H-N-S fluid geochemistry based on micro-Raman spectrometric analysis of fluid inclusions; Eur. J. Mineral., 1, 517–534.

Dubessy, J. & Ramboz, C., 1986: The history of organic nitrogen from early diagenesis to amphibolite facies: mineralogical, chemical and isotopic consequences; 5th Int. Symp. Water-Rock Interaction, Reykjavik, 171–174.

Escovar, R., 1975: Geologia y geoquimica de las minas de esmeraldas de Gachalà, Cundinamarca; Bol. Geol. (Colomb. Inst. Nac. Invest. Geol.-Min.), 22 (3), 116–153.

Forero, H.O., 1987: Esmeraldas; Publ. Geol. Ingeominas, Recursos Minerales de Colombia, 2, 557–605.

Giuliani, G., Rodriguez, C.T. & Rueda, F., 1990: Les gisements d'émeraude de la Cordillère orientale de la Colombie: nouvelles données métallogéniques; Mineral. Deposita, 25, 105–111.

Gubelin, E.J., 1957: A contribution to the genealogy of inclusions; J. Gemmol., 6, 1–47.

Guerrero, R.J. & Villanueva, A.G., 1986: Cartografia geologica y prospeccion geoquimica en la mina de esmeraldas "El Indio", Muzo, Boyacà; unpub. thesis, Univ. Nac. Bogotà, 114 p.

Guilhaumou, N., Dhamelincourt, P., Touray, J.C. & Touret, J., 1981: Étude des inclusions fluides du système N_2-CO_2 de dolomites et de quartz de Tunisie septentrionale. Données de la microcryoscopie et de l'analyse à la microsonde à effet Raman; Geochim. Cosmochim. Acta, 45, 657–673.

Kozlowski, A., Metz, P. & Jaramillo, H.A.E., 1988: Emeralds from Somondoco, Colombia: chemical composition, fluid inclusions and origin; Neues Jahrb. Mineral. Abh., 159, 23–49.

Kwak, T.A.P. 1986: Fluid inclusions in skarns (carbonate replacement deposits); J. Metamorph. Geol., 4, 363–384.

MacLaughlin, D. & Arce, M., 1971: Recursos minerales de parte de los departamentos de Cundinamarca, Boyacà y Meta; Bol. Geol. Ingeominas, 19 (1), 1–102.

Medina, L.F., 1970: Consideraciones sobre la genesis de los yacimientos esmeraldiferos de Muzo; Congr. Colombiano de Minas, 2, Manizalès, 10–20.

Oppenheim, V., 1948: The Muzo emerald zone, Colombia; Econ. Geol., 43, 31–38.

Roedder, E., 1963: Studies of fluid inclusions II: Freezing data and their interpretation; Econ. Geol., 58, 163–211.

– 1972: Composition of fluid inclusions; U.S. Geol. Surv. Prof. Pap. 440 JJ, 1–164.

– 1982: Fluid inclusions in gemstones: valuable defects; Proc. Int. Gemol. Symp., 1, Santa Monica, 479–502.

– 1984: Fluid inclusions; Rev. Mineral., 12, 644 p.

Rosasco, G.J. & Roedder, E., 1979: Application of a new Raman microprobe spectrometer to non destructive analysis of sulfate and other ions in individual phases in fluid inclusions in minerals; Geochim. Cosmochim. Acta, 43, 1907–1915.

Steward, D.B. & Potter, R.W., 1979: Application of physical chemistry of fluids in rock salt at elevated temperature and pressure to repositories for radioactive waste; in G. J. McCarthy (ed.), Scientific Basis for Nuclear Waste Management, 1, Plenum Press, New York, 297–311.

Touray, J.C. & Poirot, J.P., 1968: Observations sur les inclusions fluides primaires de l'émeraude et leurs relations avec les inclusions solides; C.R. Acad. Sci., Sér. D, 266, 305–308.

United Nations – Ingeominas, 1975: Proyecto de esmeraldas; Informe Tecnico Final, Ingeominas, 71 p. (unpub.).

Vanko, D.A., Bodnar, R.J. & Sterner, S.M., 1988: Synthetic fluid inclusions: VIII. Vapor-saturated halite solubility in part of the system NaCl-CaCl$_2$-H$_2$O with application to fluid inclusions from oceanic hydrothermal systems; Geochim. Cosmochim. Acta, **52**, 2451–2456.